Supplemental Material for "Faraday rotation enhancement of gold coated Fe2O3 nanoparticles: Comparison of experiment and theory" – Raj Kumar Dani, Hongwang Wang, Stefan H. Bossmann, Gary Wysin and Viktor Chikan, Kansas State University, June, 2010

Theory of Modeling Faraday Rotation

The Faraday rotation[1] in a medium is due to the difference of propagation of right and left circularly polarized light through it, when a magnetic field is applied along the propagation direction (z). The theory is closely related to that for optical rotation.[2] The dielectric permittivities ε_R and ε_L for the two polarizations will be slightly different, causing one polarization to be phase shifted relative to the other, after the light propagates some distance z. Once these permittivities are known for the composite medium made of core/shell particles in water, the Faraday rotation can be found.

ε_R and ε_L are the eigenvalues of the permittivity tensor in Cartesian coordinates, written as,[3]

$$\varepsilon = \begin{pmatrix} \varepsilon_{xx} & \varepsilon_{xy} \\ -\varepsilon_{xy} & \varepsilon_{xx} \end{pmatrix} \Rightarrow \text{(diagonalization)} \Rightarrow \quad \tilde{\varepsilon} = \begin{pmatrix} \varepsilon_{xx} - i\varepsilon_{xy} & 0 \\ 0 & \varepsilon_{xx} + i\varepsilon_{xy} \end{pmatrix}. \tag{1}$$

The diagonal elements are ε_R and ε_L, which gives

$$\varepsilon_{xx} = \tfrac{1}{2}(\varepsilon_R + \varepsilon_L), \quad \varepsilon_{xy} = \tfrac{i}{2}(\varepsilon_R - \varepsilon_L). \tag{2}$$

Each polarization propagates independently with a wave vector, $k_{R,L} = \dfrac{\omega}{c}\sqrt{\varepsilon_{R,L}}$. Then the Faraday rotation of linearly polarized light after propagating a distance z is found to be

$$\varphi = \tfrac{1}{2}\mathrm{Re}\{k_R - k_L\}z = \frac{\omega}{2c}\mathrm{Re}\left\{-i\frac{\varepsilon_{xy}}{\sqrt{\varepsilon_{xx}}}\right\}. \tag{3}$$

The ellipticity angle produced by the difference in extinction of the two polarizations is given instead by using the imaginary part. The Verdet constant υ is φ normalized per applied magnetic induction B and unit distance,

$$\upsilon = \varphi/(zB) = (\pi/\lambda B)\mathrm{Re}\left\{-i\varepsilon_{xy}/\sqrt{\varepsilon_{xx}}\right\}. \tag{4}$$

As ε_{xy} is proportional to B except at very high fields, υ does not depend on B. We use this approach here to get φ, based on finding the effective dielectric functions for right/left polarizations of the composite water-nanoparticle medium using a Drude model.

Dielectric Properties

The Drude model for the electron response can be used to estimate the absorption and Faraday rotation effects, due to both the Fe_2O_3 core and the gold shell. Both of these are closely related. A resonance in the absorption will correspond to a similar resonance effect in the Faraday rotation. We take the approach of finding an accurate description of the dielectric functions $\varepsilon(\omega)$, based on experimental measurements of absorption in solutions of nanoparticles. Once $\varepsilon(\omega)$ is known separately for both the core and the shell materials, the resulting Faraday rotation of core/shell nanoparticles in solution can be calculated as described below

The frequency-dependent relative dielectric permittivity of a medium, due to bound electrons at a single resonance ω_0 combined with free electrons of plasma frequency ω_p, is taken as[4] [5]

$$\varepsilon = 1 - \frac{g_0^2}{\omega^2 - \omega_0^2 + i\gamma_0\omega - \nu\omega\omega_B} - \frac{\omega_p^2}{\omega^2 + i\gamma_p\omega - \nu\omega\omega_B} \quad . \tag{5}$$

For the bound electrons, ω_0 is the binding frequency, g_0 is the oscillator strength, and γ_0 is the damping frequency. The last term in (5) represents the free electrons, with plasma frequency ω_p and damping frequency γ_p. The applied magnetic field (along *z*) responsible for the Faraday rotation enters into both terms, in the cyclotron frequency, $\omega_B = eB_z/m^*$. The helicity is $\nu = +1/-1$ for left/right circular polarization. That term, due to the Lorentz force, leads to Faraday rotation, applying expression (5) separately for both polarizations.

For the gold shell, we assume that the free electron plasma is the main contribution to ε, although a contribution from bound electrons [6] must also be included to move the plasmon frequency of gold nanoparticles into the visible. For the free electrons, we use the bulk value plasma frequency, ω_p=1.37 x 10^{16} rad/s (λ=138.5 nm), and a scattering time τ=9.1 fs, effective mass $m^* = m_e$, and damping frequency that includes scattering from the shell surfaces, [7] according to

$$\gamma_p = \frac{1}{\tau} + \frac{v_F}{d}. \tag{6}$$

The Fermi velocity is v_F=1.40 x 10^6 m/s and *d* is the thickness of the gold shell. For the bound electrons, we do not use a limiting dielectric constant like $\varepsilon_\infty \approx 10$, as in Ref. 7 to get the plasmon resonance for spherical gold particles near 530 nm. Instead, the average effect of the bound electrons is represented *approximately* by a single resonance term proportional to g_0^2 as in Eq. (5). This makes the inclusion of Faraday effects rather simple, compared to a more correct treatment of the interband transitions. The parameters have been fitted from the absorption spectrum of a solution of 17 nm diameter (average) gold nanoparticles in water (similar to that explained for γ-Fe_2O_3 parameter fitting in the following paragraph). For description of the absorption, especially near the plasmon resonance, the fitting parameters are found to be $g_0 = 4.43\times10^{15}$ rad/s, $\omega_0 = 3.86\times10^{15}$ rad/s (λ_0 =488 nm), and $\gamma_0 = 6.22\times10^{15}$ rad/s (scattering time $\tau_0 = 1/\gamma_0 = 1.61$ fs). This fit is shown in Figure 1; the fit is close to the experimental data around the plasmon resonance, and somewhat overestimates the absorption at longer wavelengths, but the model should not be taken seriously in the ultraviolet. This, however, is not

a problem, because it is the change in the frequency of the plasmon resonance with changing gold shell thickness that is responsible for many of the interesting plasmonic effects. As long as this model gives a reasonable description of that resonance, it should be able to suggest how the absorption and Faraday rotation vary with gold shell modifications.

Describing the maghemite core [γ-Fe_2O_3] is complex, because it has several different absorption resonances. There is at least one strong resonant absorption in the ultraviolet that is responsible for Faraday rotation.[8] Its tail produces the leading contribution to the absorption $\alpha(\omega)$ in the visible. The absorption spectrum of γ-Fe_2O_3 particles over 350 nm < lambda < 700 nm, not including the weaker absorption band from 460 nm -- 560 nm, was fit by using the above expression (5), see Figure 2. For a volume fraction f of spherical particles of dielectric constant ε in water (the host medium, with ε_a=1.777), the absorption is $\alpha = 2\frac{\omega}{c}\mathrm{Im}\left\{\sqrt{\varepsilon_{\mathrm{eff}}}\right\}$, where $\varepsilon_{\mathrm{eff}}$ results from the Maxwell Garnett effective medium theory[9] (MG equation),

$$\frac{\varepsilon_{\mathrm{eff}} - \varepsilon_a}{\varepsilon_{\mathrm{eff}} + 2\varepsilon_a} = f\frac{\varepsilon - \varepsilon_a}{\varepsilon + 2\varepsilon_a}. \qquad (7)$$

Assuming only bound electrons ($\omega_p = 0$) we found that g_0=5.20 x 10^{15} rad/s, ω_0=5.06 x 10^{15} rad/s (λ_0 =372 nm), and γ_0=2.89 x 10^{15} rad/s ($\tau_0 = 1/\gamma_0$=0.347 fs) describes the underlying absorption curve of Fe_2O_3 (Figure 2).[7]

The other parameters needed to describe the maghemite core are its domain saturation magnetization M = 414 kA/m, and its anisotropy constant K = 4700 J/m^3.[8] The cores have average radius b=4.85 nm, volume $V = 4\pi b^3/3$ = 478 nm^3, and magnetic moment $m = MV$, and are super-paramagnetic, as can be seen by the ratio of magnetic anisotropy energy KV= 14 meV to the thermal energy k_BT = 26 meV (at 300 K). Their average magnetic moment in an externally applied magnetic induction B follows the classical Langevin function,

$$\langle m_z \rangle = m\langle\cos\theta\rangle = m\left[\coth x - \tfrac{1}{x}\right] \approx \tfrac{1}{3}mx, \quad x \equiv \frac{mB}{k_BT}. \qquad (8)$$

For the permanent magnetization in these single domain particles, the internal magnetic field is $H_{\mathrm{in}} = -\frac{1}{3}M$ and the internal magnetic induction is $B_{\mathrm{in}} = \mu_0(H_{\mathrm{in}} + M) = \frac{2}{3}\mu_0 M$. The component along z is $B_{\mathrm{in},z} = B_{\mathrm{in}}\langle\cos\theta\rangle = \frac{2}{3}\mu_0 M\frac{x}{3} = \left(\frac{2}{9}\mu_0 VM^2/k_BT\right)B$. This internal magnetic induction is amplified by the factor $\left(\frac{2}{9}\mu_0 VM^2/k_BT\right)$ = 5.5, which helps to enhance the Faraday rotation compared to that in a non-magnetized medium.

For pure particles of either gold or maghemite in a water solution, the MG theory (7) can be applied to calculate the Faraday rotation. Figure 3 indicates how the plasmon peak in $\alpha(\omega)$ for gold is accompanied by a similar peak in the Verdet function, $\upsilon(\omega)$. Further, the plasmon width increases for smaller particles, due to the enhanced surface scattering term.

Core/shell particle's permittivity ε_s

The individual particles are assumed to be spherical, with a maghemite core (ε_c) of radius b, surrounded by a shell of gold (ε_b) to outer radius a, much less than the wavelength of light being considered. The particle is immersed in a medium (water) with dielectric constant ε_a. From

their separate frequency-dependent permittivities, we require first the effective permittivity of one spherical particle, ε_s. This can be found equivalently either by (1) finding the effective polarization and average internal electric field using electrostatics, or (2) applying Maxwell Garnett theory[9, 10] to a single particle, taking the Fe_2O_3 core as an inclusion of internal volume fraction $f_c = (b/a)^3$ within the gold shell "host" medium. The composite particle's dielectric function ε_s is found to be

$$\varepsilon_s = \varepsilon_b \frac{1+2\beta_c}{1-\beta_c}, \quad \beta_c = f_c \frac{\varepsilon_c - \varepsilon_b}{\varepsilon_c + 2\varepsilon_b}, \quad f_c = (b/a)^3. \text{ (9, Solution of MG equation.)}$$

This effective permittivity is also expressed as $\varepsilon_s = \varepsilon_b + \alpha_s / F_s$, where the susceptibility and internal field per applied field of a spherical particle surrounded by a host medium ε_a are found via electrostatics as

$$\alpha_s = \frac{\langle P_{\text{in}} \rangle}{E_0} = 3\varepsilon_a \frac{\varepsilon_s - \varepsilon_a}{\varepsilon_s + 2\varepsilon_a}, \qquad F_s = \frac{\langle E_{\text{in}} \rangle}{E_0} = \frac{3\varepsilon_a}{\varepsilon_s + 2\varepsilon_a}. \tag{10}$$

Effective Composite Medium

These particles are dispersed into water with a volume fraction $f_s = n_s V_s$, where $n_s \approx 3.5 \times 10^{18}/\text{m}^3$ is their number density and $V_s = 4\pi a^3/3$ is their volume that depends on the outer radius of the gold shell. We consider two different ways to determine the effective permittivity of the solution: (1) Maxwell Garnett effective medium theory, assuming that the spheres are well separated and scatter light independently; (2) Bruggeman theory,[9, 10] supposing that the spheres combine into clusters composed from hundreds to thousands of the core/shell particles in a closed packed arrangement with a volume fraction $f_{\text{Br}} \approx 0.74$.

In the MG theory the effective permittivity of the composite can be expressed as

$$\varepsilon_{\text{eff}} = \varepsilon_a + f_s \alpha_s / [1 - f_s(1 - F_s)] \quad \text{or as} \quad \varepsilon_{\text{eff}} = \varepsilon_a \frac{1+2\beta_s}{1-\beta_s}, \quad \beta_s = f_s \frac{\varepsilon_s - \varepsilon_a}{\varepsilon_s + 2\varepsilon_a}. \tag{11}$$

This expression is evaluated separately for left/right polarizations, from which the Faraday rotation can be found using (2) and (3). Some results for absorption and Faraday rotation due to core/shell particles are shown in Figure 4. The important aspect of the results is that the plasmon resonance starts at long wavelengths for very thin gold shells, and moves towards about 520 nm with increasing shell thickness. Note that the volume fraction f_s increases with thickness of the gold shell, as the number density of particles was nearly constant in experiments.

To include the clustering effects via the Bruggeman theory, we first find the effective permittivity of a cluster, ε_{cl}, composed from volume fraction f_{Br} of core/shell spheres surrounded by volume fraction $1 - f_{\text{Br}}$ of water host (ε_a). The cluster effective permittivity ε_{cl} solves the Bruggeman equation,

$$f_{\text{Br}} \frac{\varepsilon_s - \varepsilon_{cl}}{\varepsilon_s + 2\varepsilon_{cl}} + (1 - f_{\text{Br}}) \frac{\varepsilon_a - \varepsilon_{cl}}{\varepsilon_a + 2\varepsilon_{cl}} = 0, \tag{12}$$

where the first term represents the contribution of the spheres surrounded by averaged cluster, and the second term represents the water surrounded by averaged cluster. The solution for the effective permittivity of a cluster is found to be

$$\varepsilon_{cl} = \tfrac{1}{4}\left\{(2-3f_{\mathrm{Br}})\varepsilon_a + (3f_{\mathrm{Br}}-1)\varepsilon_s + \sqrt{\left[(2-3f_{\mathrm{Br}})\varepsilon_a + (3f_{\mathrm{Br}}-1)\varepsilon_s\right]^2 + 8\varepsilon_a\varepsilon_s}\right\}. \quad (13)$$

It is interesting to note that the limit $f_{\mathrm{Br}} = 1$ of this Bruggeman cluster effect just recovers the simpler MG result (i.e., Eq. (12) gives $\varepsilon_{cl} = \varepsilon_s$). Both theories predict the blue shift of the plasmon resonance in the absortion spectrum with increasing gold shell thickness (Figures 4 and 5).

Once $\varepsilon_{\mathrm{cl}}$ is found, we again apply MG theory to get $\varepsilon_{\mathrm{eff}}$ due to these clusters dispersed at a low volume fraction f_{cl} in the water (for both left/right polarizations). [Note: At low volume fraction, the MG and Bruggeman theories give the same effective permittivity.] The number density of clusters in the water is $n_{\mathrm{cl}} = n_s/N_s$, where $N_s = f_{\mathrm{Br}}V_{\mathrm{cluster}}/V_s$ is the number of core/shell spheres in a cluster. Then the volume fraction of clusters in the water is $f_{\mathrm{cl}} = n_{\mathrm{cl}}V_{\mathrm{cluster}} = f_s/f_{\mathrm{Br}}$. This does not depend on the size of the cluster, just on its packing density. The final application of the MG theory gives the effective permittivity of the composite medium,

$$\varepsilon_{\mathrm{eff}} = \varepsilon_a\frac{1+2\beta_{cl}}{1-\beta_{cl}}, \quad \beta_{cl} = f_{cl}\frac{\varepsilon_{cl}-\varepsilon_a}{\varepsilon_{cl}+2\varepsilon_a}. \quad (14)$$

This is used in Eqs. (2) and (3) to get the Faraday rotation, including the clustering effects. Although the clusters have typical sizes from 80 nm to 160 nm across, only their internal packing fraction was needed in the theory, not their size.

Figure 5 shows the results of using a cluster packing fraction f_{Br} =0.7, close to the hard sphere value. Although clustering effects are probably important, such a large value of packing fraction does not fit the peak in the absorption very well, as seen in Figure 6; both the absorption and Faraday rotation plasmon peaks fall at a wavelength that is too long. In fact the absorption peak's position with shell thickness is better fitted using $f_{\mathrm{Br}} \approx 0.035$ as seen in Fig. 6. Further, the net Faraday rotation [Eq. (3)] and Verdet constant [Eq. (4)] are proportional to the particle volume fraction, f_s, when $f_s << 1$. Thus, some results are presented for the Verdet constant normalized by volume fraction, υ/f_s, as shown in Fig. 7. The experimentally measured Faraday rotation seems to be more consistent with the clustering model at a fairly large packing fraction like 70%. However, probably a more complete description of nanoparticle interactions is needed to consistently describe both the absorption and Faraday rotation spectra of these nanoparticle solutions simultaneously.

Nevertheless, this calculation shows that the blue-shifting of the gold plasmon peak with increasing gold shell thickness is reflected in the Faraday rotation spectrum, as seen in the downward peak in Figure 7. The strength of the clustering or other interparticle interactions or interference terms can be expected to modify the magnitude and width of this downward peak, but regardless of these details, it is ultimately linked to the blue-shifting of the gold plasmon mode.

Supplemental References

1. Hecht, E., Optics. **1997**, 366-368.
2. Jones, L. L.; Eyring, H., A Model for Optical-Rotation. *J. Chem. Educ.* **1961,** 38, (12), 601-&.
3. Xia, T. K.; Hui, P. M.; Stroud, D., Theory of Faraday-Rotation in Granular Magnetic-Materials. *Journal of Applied Physics* **1990,** 67, (6), 2736-2741.
4. Palik, E. D.; Henvis, B. W., A Bibliography of Magnetooptics of Solids. *Appl. Opt.* **1967,** 6, (4), 603-603.
5. Jackson, J. D., *Electrodynamics*. 1998.
6. Scaffardi, L. B.; Tocho, J. O., Size dependence of refractive index of gold nanoparticles. *Nanotechnology* **2006,** 17, (5), 1309-1315.
7. Antoine, R.; Brevet, P. F.; Girault, H. H.; Bethell, D.; Schiffrin, D. J., Surface plasmon enhanced non-linear optical response of gold nanoparticles at the air/toluene interface. *Chemical Communications* **1997**, (19), 1901-1902.
8. Tepper, T.; Ilievski, F.; Ross, C. A.; Zaman, T. R.; Ram, R. J.; Sung, S. Y.; Stadler, B. J. H., Magneto-optical properties of iron oxide films. *Journal of Applied Physics* **2003,** 93, (10), 6948-6950.
9. Mallet, P.; Guerin, C. A.; Sentenac, A., Maxwell-Garnett mixing rule in the presence of multiple scattering: Derivation and accuracy. *Phys. Rev. B* **2005,** 72, (1).
10. Bruggeman, D. A. G., Berechnung verschiedener physikalischer Konstanten von heterogenen Substanzen. II. Dielektrizitätskonstanten und Leitfähigkeiten von Vielkristallen der... *Annalen der Physik* **1936,** 417, (7).

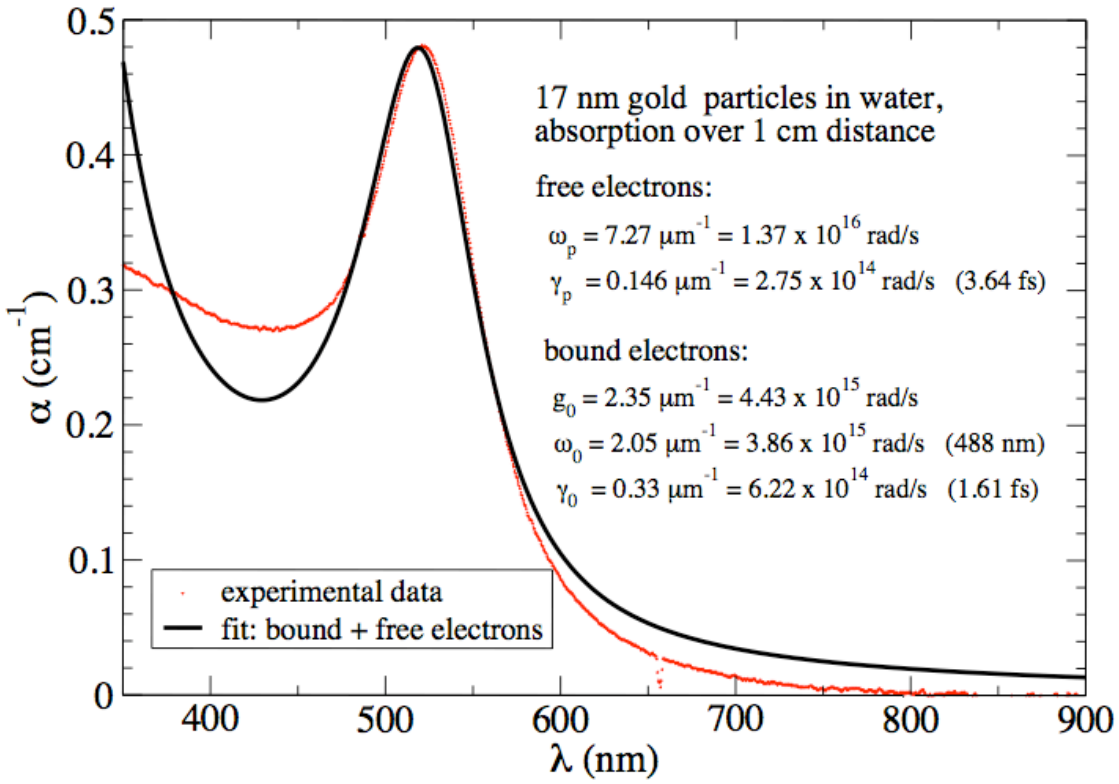

Figure 1. Fit of experimentally measured absorption of gold nanoparticle solution to model dielectric function including both free and bound electrons.

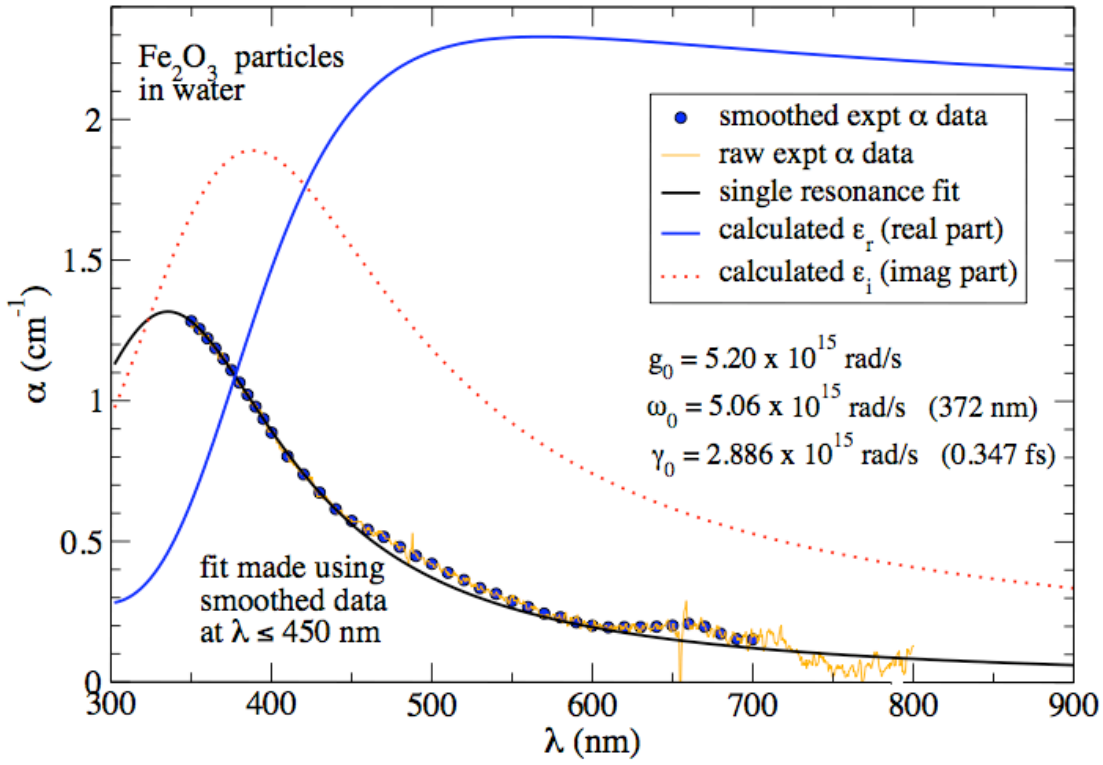

Figure 2. Fit of absorption spectrum of maghemite nanoparticles in water solution for determining its dielectric function. The real and imaginary parts of the resulting $\varepsilon(\lambda)$ are also shown.

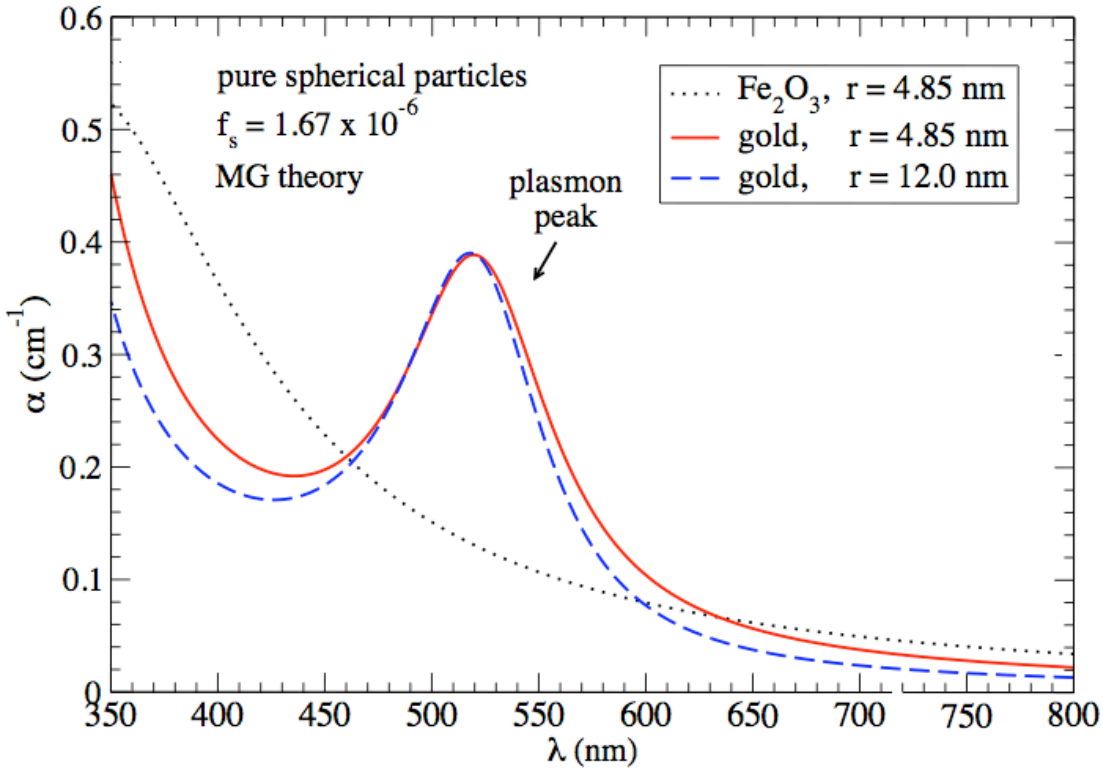

Figure 3a. Absorption (a) and Faraday rotation or Verdet constant (b) calculated for nanoparticles indicated, in water solution, using the Maxwell Garnett theory at a volume fraction $f_s = 1.67 \times 10^{-6}$. The plasmon resonance appears clearly in both quantities, and is wider for smaller particles.

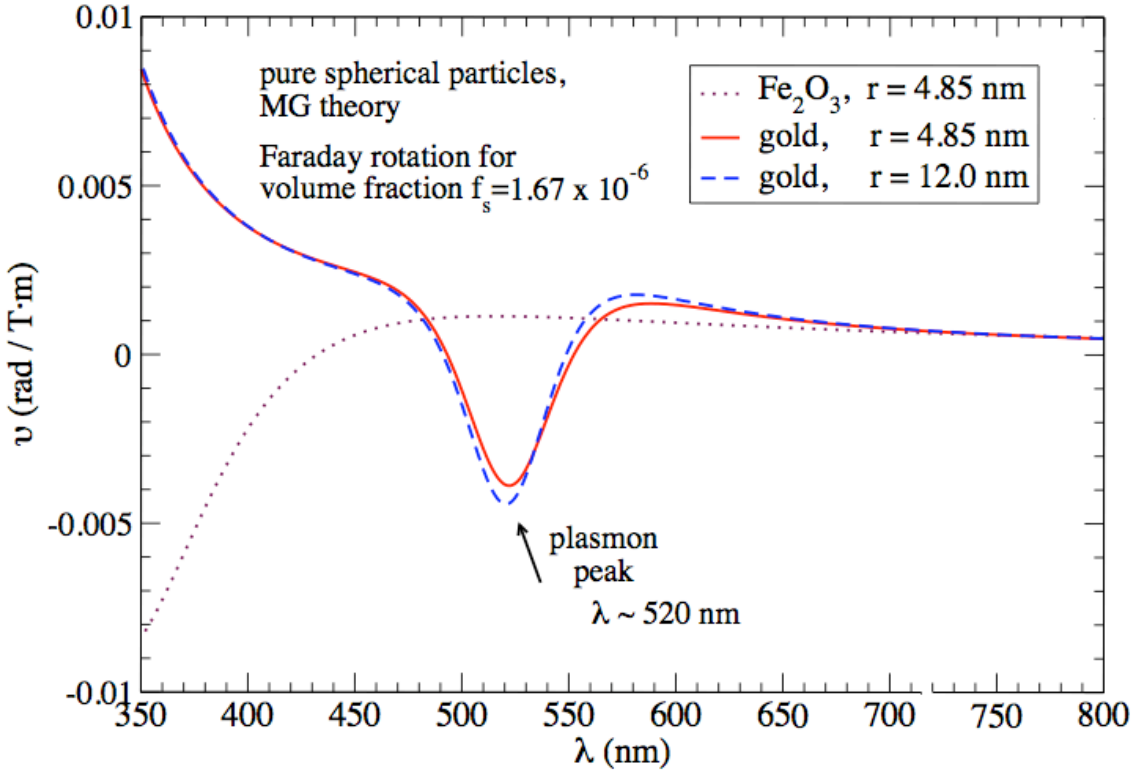

Figure 3b. Absorption (a) and Faraday rotation or Verdet constant (b) calculated for nanoparticles indicated, in water solution, using the Maxwell Garnett theory at a volume fraction $f_s = 1.67 \times 10^{-6}$. The plasmon resonance appears clearly in both quantities, and is wider for smaller particles.

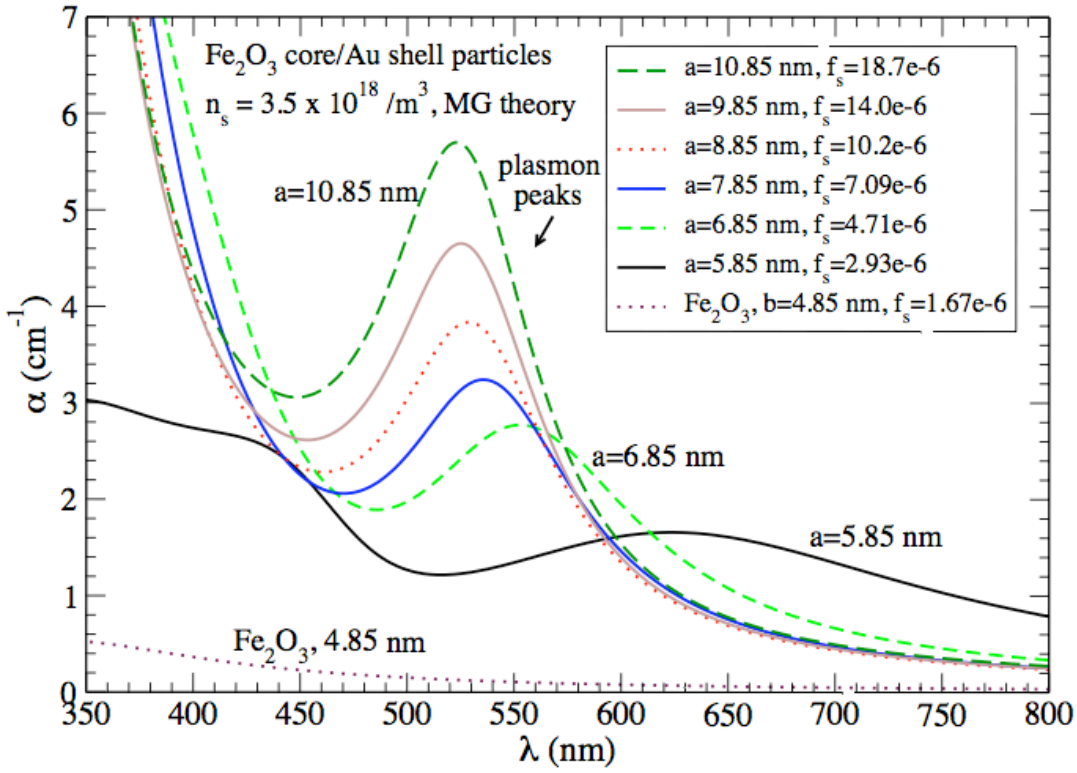

Figure 4a. Absorption (a) and Faraday rotation (b) for core/shell nanoparticles in water, showing the variations with increasing gold shell thickness. Notably, the plasmon peak moves towards shorter wavelength with increasing shell thickness.

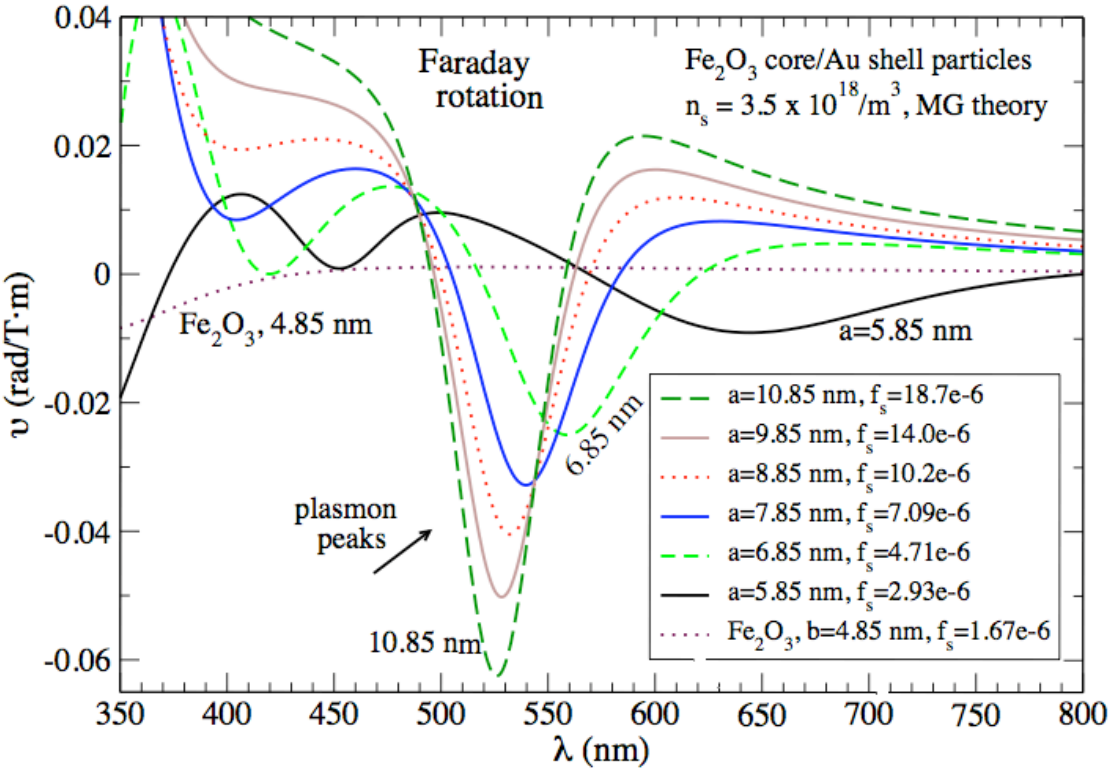

Figure 4b. Absorption (a) and Faraday rotation (b) for core/shell nanoparticles in water, showing the variations with increasing gold shell thickness. Notably, the plasmon peak moves towards shorter wavelength with increasing shell thickness.

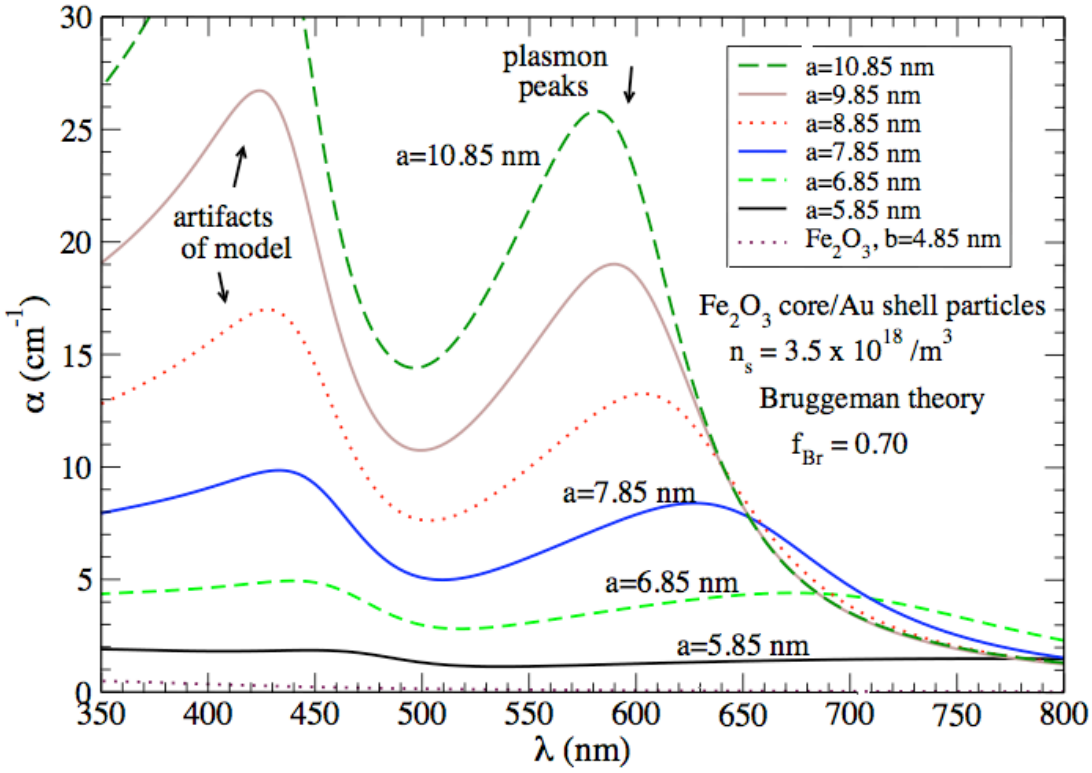

Figure 5a. Absorption (a) and Faraday rotation (b) for core/shell particle solutions in water, including strong clustering effects via the Bruggeman theory. The peaks below 450 nm are artifacts due to the single resonance assumed for bound gold electrons. The plasmon peak is slightly higher than that found without clustering effects.

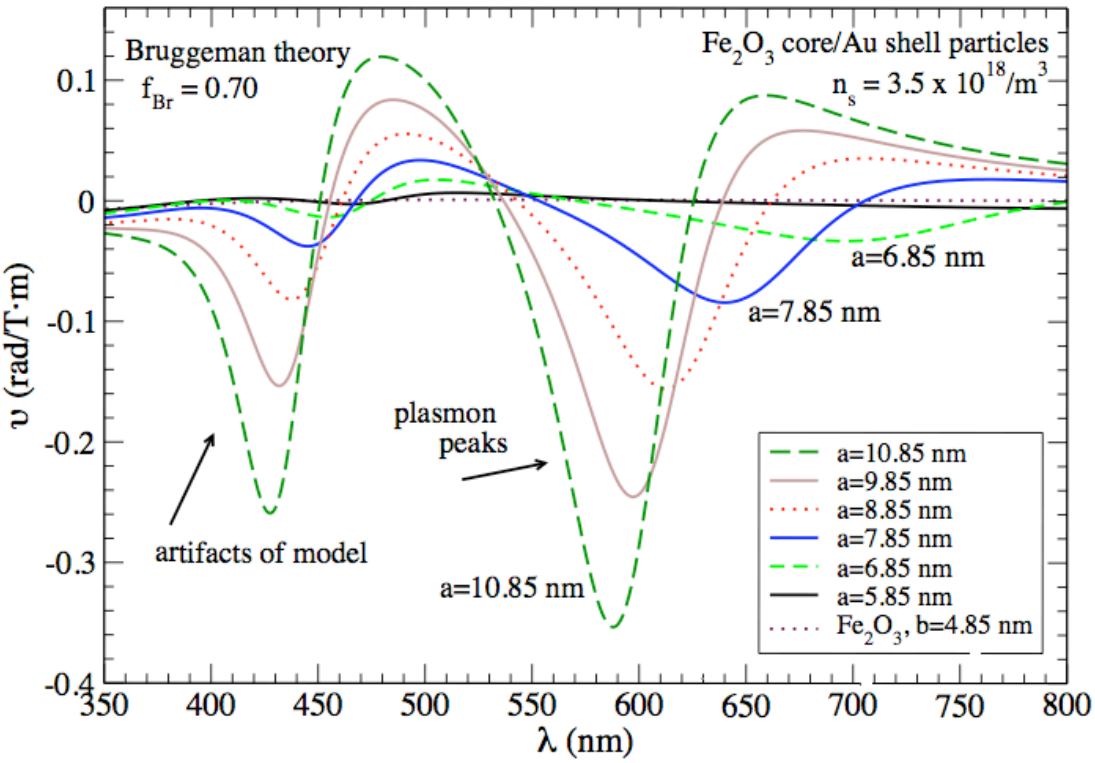

Figure 5b. Absorption (a) and Faraday rotation (b) for core/shell particle solutions in water, including strong clustering effects via the Bruggeman theory. The peaks below 450 nm are artifacts due to the single resonance assumed for bound gold electrons. The plasmon peak is slightly higher than that found without clustering effects.

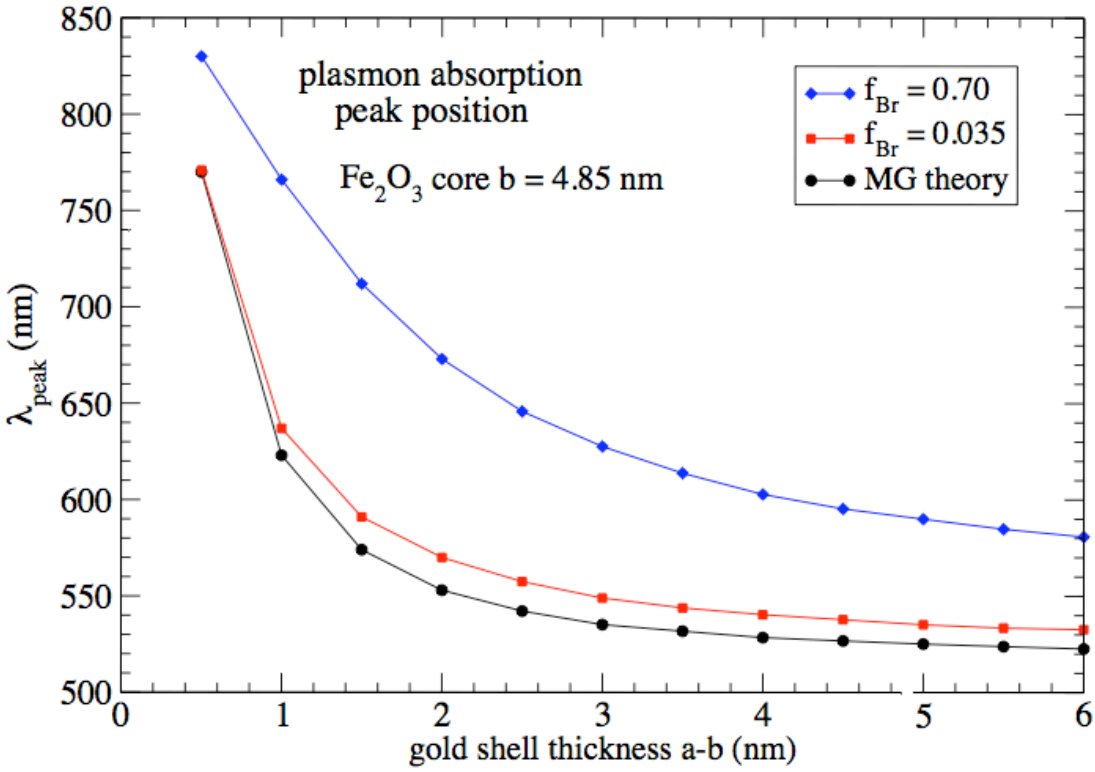

Figure 6a. Comparison of different clustering levels, showing (a) the position of the gold plasmon absorption peak and (b) the absorption of nanoparticle solution at 633 nm with increasing gold shell thickness. The Maxwell Garnett theory does not include clustering effects.

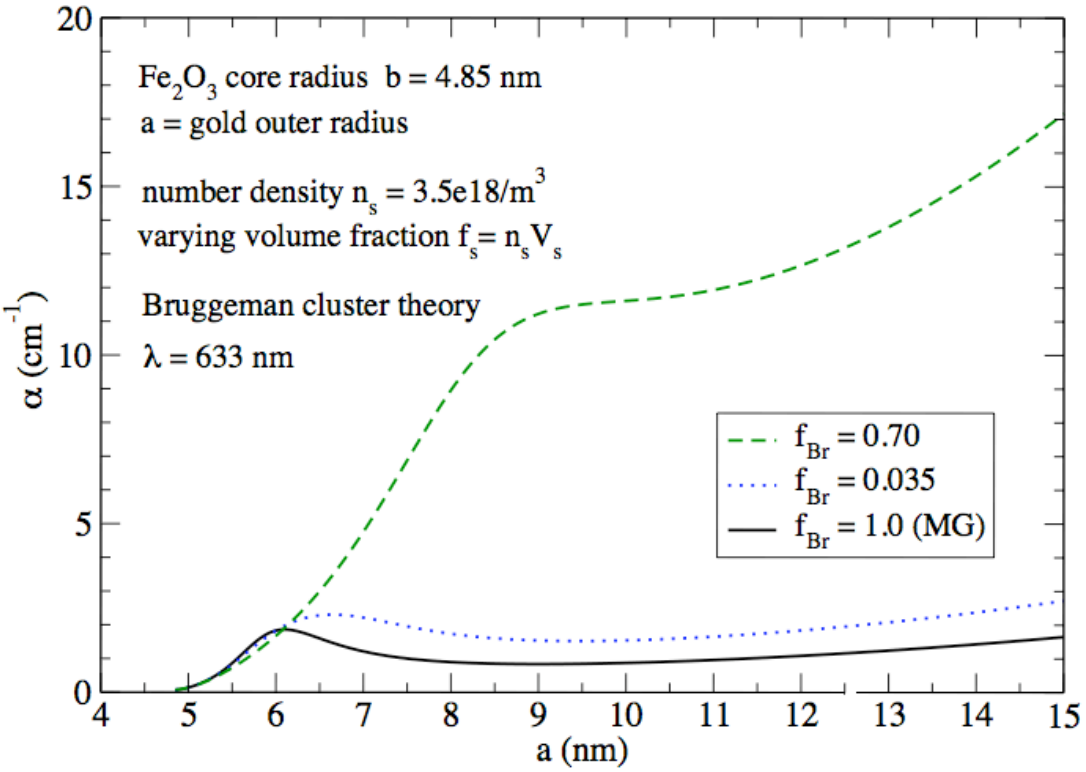

Figure 6b. Comparison of different clustering levels, showing (a) the position of the gold plasmon absorption peak and (b) the absorption of nanoparticle solution at 633 nm with increasing gold shell thickness. The Maxwell Garnett theory does not include clustering effects.

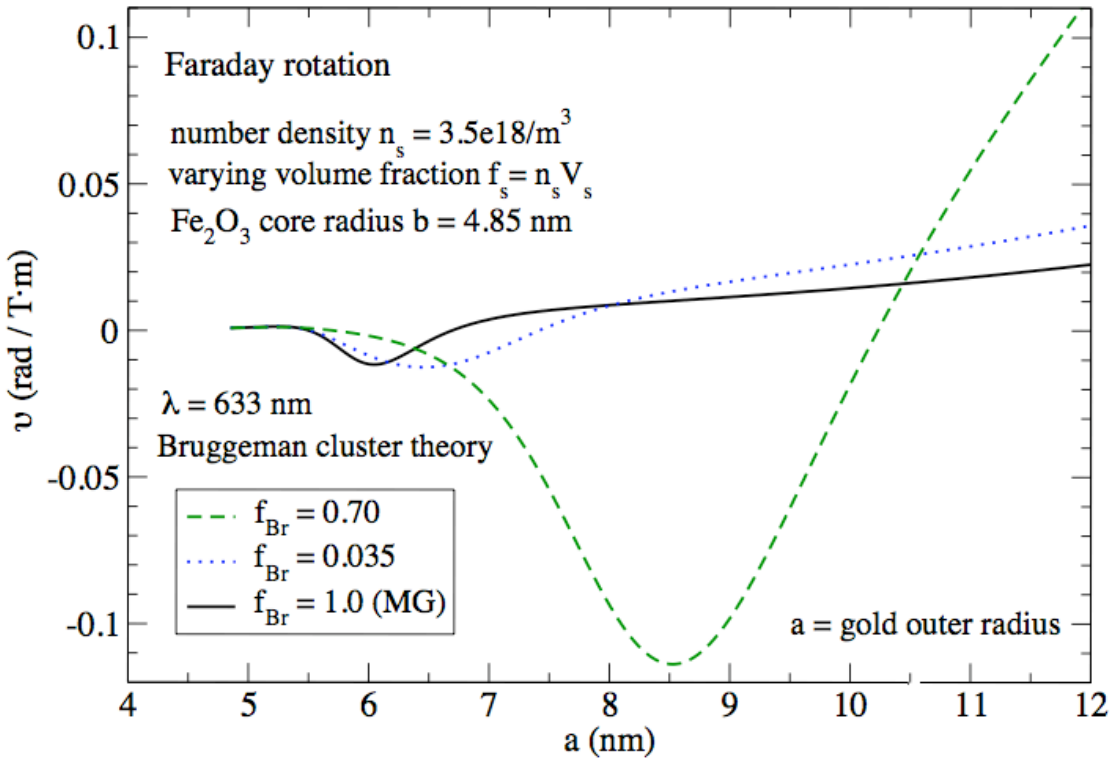

Figure 7a. Effect of clustering strength on Faraday rotation at 633 nm, using the Bruggeman theory. Part (a) shows the Verdet constant with increasing gold shell thickness. Part (b) shows the Verdet constant normalized by the volume fraction of spherical nanoparticles.

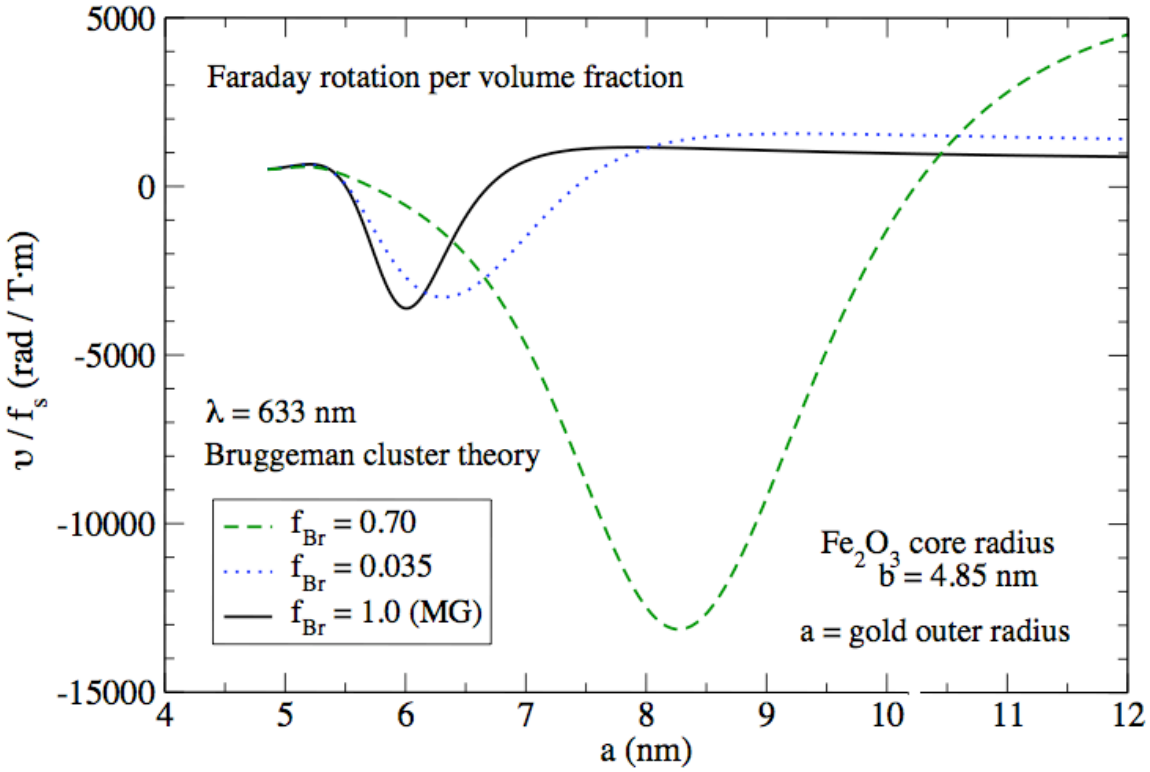

Figure 7b. Effect of clustering strength on Faraday rotation at 633 nm, using the Bruggeman theory. Part (a) shows the Verdet constant with increasing gold shell thickness. Part (b) shows the Verdet constant normalized by the volume fraction of spherical nanoparticles.